

Performance of a Shell-and-Tube Heat Exchanger with Spiral Baffle Plates

Young-Seok Son*, Jee-Young Shin

School of Mechanical and Industrial System Engineering, Dong-Eui University, Busan 614-714, Korea

In a conventional shell-and-tube heat exchanger, fluid contacts with tubes flowing up and down in a shell, therefore there is a defect in the heat transfer with tubes due to the stagnation portions. Fins are attached to the tubes in order to increase heat transfer efficiency, but there exists a limit. Therefore, it is necessary to improve heat exchanger performance by changing the fluid flow in the shell. In this study, a highly efficient shell-and-tube heat exchanger with spiral baffle plates is simulated three-dimensionally using a commercial thermal-fluid analysis code, CFX4.2. In this type of heat exchanger, fluid contacts with tubes flowing rotationally in the shell. It could improve heat exchanger performance considerably because stagnation portions in the shell could be removed. It is proved that the shell-and-tube heat exchanger with spiral baffle plates is superior to the conventional heat exchanger in terms of heat transfer.

Key Words : Shell-and-Tube Heat Exchanger, Conventional Vertical Baffle Plate, Spiral Baffle Plate, Heat Transfer, Three-Dimensional Numerical Analysis

Nomenclature

A	: Area
\vec{B}	: Body force
H	: Total enthalpy
h	: Static enthalpy
k	: Thermal conductivity
P	: Pressure
Q	: Heat transfer rate
T	: Temperature
t	: Time
\vec{U}	: Velocity vector
U	: Velocity in x -direction, overall heat transfer coefficient
V	: Velocity in y -direction
W	: Velocity in z -direction
ΔT_{lm}	: Log mean temperature difference

Greek symbols

δ	: Kronecker delta
----------	-------------------

μ	: Viscosity
ρ	: Density
σ	: Stress tensor
ξ	: Bulk viscosity

Subscripts

c	: Cold
h	: Hot
i	: Inlet
o	: Outlet
s	: Solid

Superscripts

T	: Transpose
-----	-------------

1. Introduction

Heat exchangers are devices that provide the flow of thermal energy between two or more fluids at different temperatures. Heat exchangers are used in a wide variety of applications. These include power production, process, chemical, and food industries, electronics, environmental engineering, waste heat recovery, manufacturing industry, and air-conditioning, refrigeration and space applications.

* Corresponding Author,

E-mail : ysson@dongeui.ac.kr

TEL : +82-51-890-1648; FAX : +82-51-890-2232

School of Mechanical and Industrial System Engineering, Dong-Eui University, Busan 614-714, Korea. (Manuscript Received March 2, 2001; Revised August 20, 2001)

There are many types of heat exchangers. A typical double-pipe heat exchanger consists of one pipe placed concentrically inside another of larger diameter with appropriate fittings to direct the flow from one section to the next. Shell-and-tube heat exchangers are built of round tubes mounted in a cylindrical shell with the tubes parallel to the shell. One fluid flows inside the tubes, while the other fluid flows across and along the axis of the shell. They offer great flexibility to meet almost any service requirement. They can be designed for high pressure difference between fluid streams. They are widely used in process industries, in conventional and nuclear power plants as condensers, in pressurized water reactors as steam generators, in feed water heaters, and in some air-conditioning and refrigeration systems (Incropera and DeWitt, 1996; Walker, 1990). The thermal and flow analyses of heat exchangers have been performed (Lee, K. S. *et al.*, 1998; Lee and Kim, 1999; Lee, S. H. *et al.*, 1998).

In shell-and-tube heat exchangers, baffles are installed in the shell side to increase the convection heat transfer coefficient of the shell side fluid by inducing turbulence and a cross-flow velocity component. Also, importantly, baffles support tubes for structural rigidity, preventing tube vibration and sagging. The flow and heat transfer characteristics of a conventional shell-and-tube heat exchanger have been studied experimentally (Gay *et al.*, 1976; Lee *et al.*, 1997; Shah and Pignotti, 1997; Li and Kottke, 1998a; Sparrow and Reifschneider, 1986; Li and Kottke, 1998b) and numerically (Prithiviraj and Andrews, 1998a; Prithiviraj and Andrews, 1998b). The stagnation area occurring near the contact regions of the shell and baffles in a conventional shell-and-tube heat exchanger has a detrimental effect on the heat transfer between the shell and tube side fluids. This can be overcome by extended surfaces on the tube side, which has a limitation.

The efforts to improve the shell side flow characteristics are made using the spiral baffle plates instead of vertical baffle plates. Therefore, the new design of the shell-and-tube heat exchanger with spiral baffle plates are proposed

to eliminate the stagnation area in the shell side flow in a conventional shell-and-tube heat exchanger. Rotational flow in the shell side caused by the spiral baffle plates eliminates the stagnation area and improves the heat transfer significantly. In this paper, three-dimensional numerical analyses are performed for the shell-and-tube heat exchanger with spiral baffle plates using the commercial CFD program, CFX4. 2 (AEA Technology, 1997). Shell-side and tube-side flow fields, pressure drop, and heat transfer performance are analyzed. These results are compared with those of the conventional shell-and-tube heat exchanger.

2. Numerical Analysis

2.1 Model

Shell-and-tube heat exchangers are built of round tubes mounted in a large cylindrical shell with the tube axis parallel to that of the shell. In a conventional shell-and-tube heat exchanger with vertical baffles, the shell side stream flows across pairs of baffles, and then flows parallel to the tubes as it flows from one baffle compartment to the next as shown in Fig. 1.

The stagnation area occurring in a conventional shell-and-tube heat exchanger has an unfavorable effect on the heat transfer between the shell- and tube-side fluids. The spiral baffle plate is one of the methods to improve the shell side flow characteristics. The baffle has a spiral shape like a screw and does not have baffle cut as depicted in Fig. 2. The three quarters portion of a spiral baffle is manufactured from a solid die, and the holes for tubes are not made perpendicular to

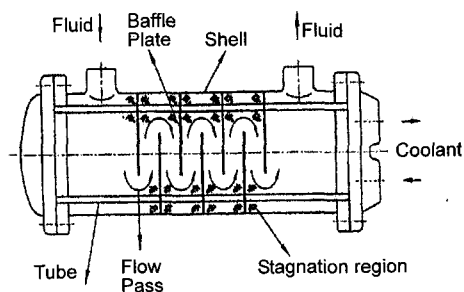


Fig. 1 Conventional shell-and-tube heat exchanger

Table 1 Specifications of the current model (in mm)

		Conventional	Spiral
Shell	diameter	114.3	114.3
	length	667	667
Tube	diameter	28.4	28.4
	thickness	2	2
Baffle	No.	7	7
	thickness	2	2
	spacing	72	72

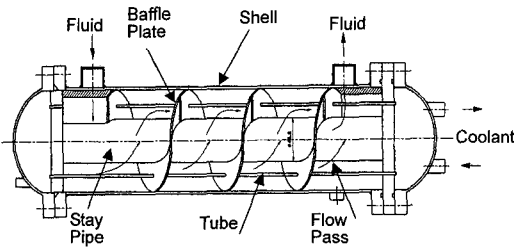


Fig. 2 Shell-and-tube heat exchanger with spiral baffle plates

the surface of the baffle but to the vertical plane (holes at the surface are oval). The spiral baffles are made by riveting the three quarters spiral baffles successively. Flow in the shell side rotates circumferentially along the spiral baffle plate, and it contributes the elimination of the stagnation area and enhancement of the heat transfer significantly.

Figure 3 shows the basic model with 7 spiral baffle plates of this study. The inter-baffle spacing is 72 mm, and the physical dimensions are same as those of the conventional heat exchanger, shell diameter and axial length of 114.3 mm and 667 mm, tube diameter and thickness of 28.4 mm and 2 mm. Refer to Table 1 for the details. One shell pass and four tube passes system is assumed, and there is one tube per tube pass.

2.2 Governing equations and boundary conditions

The model uses conservation of mass, momentum, and energy principles (AEA Technology, 1997).

The continuity relation is

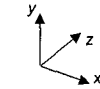
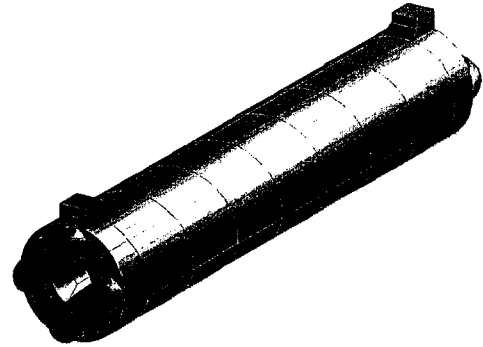


Fig. 3 (a) Schematic view of the shell-and-tube heat exchanger with spiral baffle plates (external view)

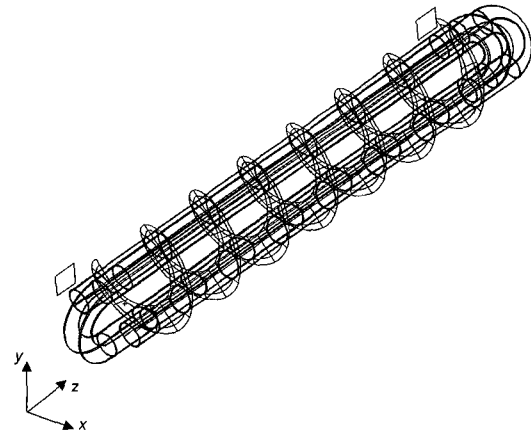


Fig. 3 (b) Schematic view of the shell-and-tube heat exchanger with spiral baffle plates (internal view)

$$\frac{\partial \rho}{\partial t} + \nabla \cdot (\rho \vec{U}) = 0 \tag{1}$$

The general momentum equation is

$$\frac{\partial \rho \vec{U}}{\partial t} + \nabla \cdot (\rho \vec{U} \times \vec{U}) = -\vec{B} + \nabla \cdot \sigma \tag{2}$$

where σ is the stress tensor as in Eq. (3).

$$\sigma = -P\delta + \left(\xi - \frac{2}{3}\mu \right) \nabla \cdot \vec{U} \delta + \mu (\nabla \vec{U} + (\nabla \vec{U})^T) \tag{3}$$

where ρ is the fluid density, \vec{U} is the fluid velocity, P is the pressure, and t is the time. \vec{B} is the body force, μ is the viscosity, and ξ is the bulk viscosity. The k - ϵ turbulence model is included.

Table 2 Boundary conditions

		Unit	Laminar	Turbulent
Tube inlet	U, V	m/s	0	0
	W	m/s	0.07893	0.7893
	T	K	303.15	303.15
Tube outlet	P	Pa	0	0
Shell inlet	U, W	m/s	0	0
	V	m/s	-0.03316	-0.3316
	T	K	373.15	373.15
Shell outlet	P	Pa	0	0

The energy equation is described in Eq. (4).

$$\frac{\partial \rho H}{\partial t} + \nabla \cdot (\rho \bar{U} H) - \nabla \cdot (k \nabla T) = \frac{\partial P}{\partial t} \quad (4)$$

where H is the total enthalpy (static enthalpy plus kinetic energy) as shown in Eq. (5), h is the static enthalpy, T is the temperature, and k is the thermal conductivity.

$$H = h + \frac{1}{2} \bar{U}^2 \quad (5)$$

Thermodynamic equations of state are added to solve these sets of equations as $\rho = \rho(T, P)$, $h = h(T, P)$. Heat diffusion equation for solid region is as follows:

$$\frac{\partial}{\partial t} (\rho_s H) - \nabla \cdot (k_s \nabla T) = 0 \quad (6)$$

Orthogonal coordinate system and body fitted grid are used for computation. Also, incompressible steady flow is assumed. Uniform velocity and temperature are given for inlet conditions. Outlet pressure is given, and the gradients of other variables at outlet are set to zero. Velocity for turbulent case is set as ten times higher than that of laminar case. Boundary conditions are summarized in Table 2, and water flows in both tube and shell sides.

Finite volume method (Patankar, 1980) is used, and the SIMPLEC (SIMPLE Corrected) method (Van Doormaal and Raithby, 1984) is employed. The discretized equations are underrelaxed using the relaxation factors 0.7 and 0.65 for temperature and velocity, respectively. Non-staggered grid and multi-block grid structures are employed. During computation, it

is assumed that the convergence is reached when the error in continuity, the mass source residual, has fallen below 0.1.

3. Results

To select appropriate number of cells guaranteeing accuracy and efficient computation time of the analysis, grid independence study has been performed. Table 3 shows the effects of the number of cells on the results. The calculations were performed on a SUN ULTRA5 workstation. Among the coarse, intermediate, and fine grids, intermediate grid was selected considering both the accuracy of the solution and the computation time. As seen in Table 3, the coarse grid provides small error in the mass and enthalpy balance at inlet and outlet, however, the differences in those values between the coarse grid and the intermediate grid is so significant. Fine grid shows relatively large error in enthalpy balance because the number of iteration was limited considering the excessive computation time. Intermediate grid system offers nearly same values as those of fine grid system, and relatively small error in the enthalpy balance. The grid shape is also important in the accuracy of the solution. CFX4.2 employs multi-block grid structures and uses elliptic smoothing which provides smooth meshes to ensure good grids of smoothness and near orthogonality (AEA Technology, 1997).

Figure 4 shows velocity vectors on a transverse plane at $X=0.023$ m and $Z=0.237 \sim 0.478$ m of a conventional shell-and-tube heat exchanger. This plane shows the two tubes and the shell-side flow field, which is moved by 0.023 m from the center in the radial direction. As seen in Fig. 4, the tube-side fluid flows at nearly uniform velocity. The shell-side fluid flows up-and-down along the baffle plates. However, it flows parallel to the tubes within a baffle window, because the resistance is lower in the axial direction compared with the cross-flow direction. Stagnation occurs near the contact regions of the shell and baffle plates, which could partially explain the ineffectiveness of the heat transfer in the conventional heat exchanger.

Table 3 Summary of grid independence study

No. of cells	No. of iteration	Computation time (days)	Mass balance (kg/s)			Energy balance (W)		
			Inlet	Outlet	Error (%)	Inlet	Outlet	Error (%)
166,976	600	7	0.5643	0.5643	0.0	94855	93717	1.2
214,208	1400	18	0.3069	0.3069	0.0	75370	74710	0.8
276,540	1000	21	0.3070	0.3070	0.0	75370	71080	5.6

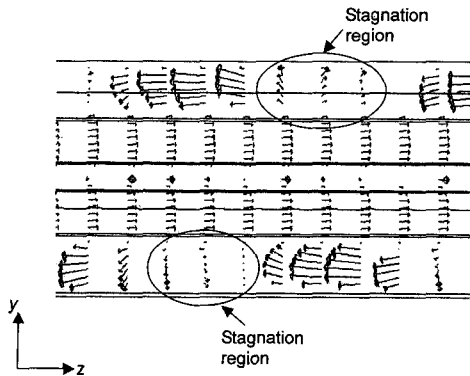


Fig. 4 Velocity vectors on a transverse plane - with conventional baffle ($X=0.023$, $Z=0.237\sim 0.478$)

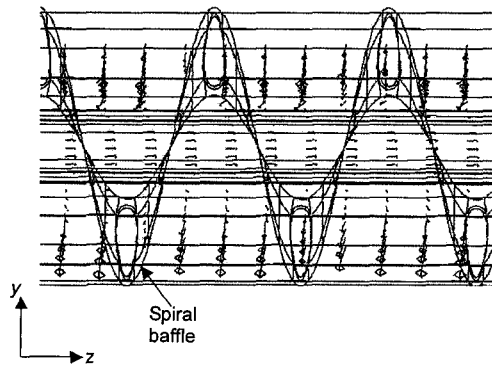


Fig. 5 Velocity vectors on a transverse plane - with spiral baffle ($X=0.037$, $Z=0.241\sim 0.435$)

Figure 5 shows velocity vectors on a transverse plane at $X=0.037$ m and $Z=0.241 \sim 0.435$ m of a shell-and-tube heat exchanger with spiral baffle plates. This plane shows the one tube and the shell-side flow field. The shell-side fluid flows along the spiral baffle plates accompanying rotation. The magnitude of the velocity vector is very small because only the component in this plane could be seen. However, it is also the

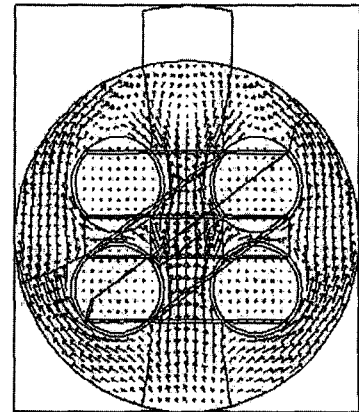


Fig. 6 Velocity vectors on a cross-sectional plane - with conventional baffle ($Z=0.15$)

evidence of the rotation of the flow field itself along the spiral baffle plates. Stagnation area seems to be reduced evidently as compared with the conventional shell-and-tube heat exchanger.

Figure 6 shows velocity vectors of a conventional shell-and-tube heat exchanger on a vertical plane at $Z=0.15$ m. Again we could observe that the shell-side fluid flows up-and-down along the baffles, and the maximum velocity occurs at the baffle window. The flow field at the bottom of the shell is quite stable in this cross-section, so the heat transfer enhancement is not substantial.

For the shell-and-tube heat exchanger with spiral baffle plates, the velocity vectors on a vertical plane to the axis at $Z=0.19$ m are shown in Fig. 7. The shell-side fluid flows along the spiral baffles, and the fluid accelerates at the narrow space between the tube and the shell. The flow vorticity occurring between the tubes

Table 4 Comparison of the performance of the shell-and-tube heat exchanger with conventional and spiral baffle plates

	Type of baffle	Conventional		Spiral	
	No. of baffles	7		7	
	Flow	Laminar	Turbulent	Laminar	Turbulent
Shell side	Inlet temp. ($T_{h,i}$), K	373.15	373.15	373.15	373.15
	Outlet temp. ($T_{h,o}$), K	369.55	369.77	369.11	368.64
	Inlet pressure ($P_{h,i}$), Pa	669	67900	9880	980000
	Outlet pressure ($P_{h,o}$), Pa	0	0	0	0
	Temp. drop (ΔT_h), K	3.60	3.38	4.04	4.51
	Pressure drop (ΔP_h), Pa	669	67900	9880	980000
Tube side	Inlet temp. ($T_{c,i}$), K	303.15	303.15	303.15	303.15
	Outlet temp. ($T_{c,o}$), K	325.90	324.13	324.30	326.76
	Inlet pressure ($P_{c,i}$), Pa	21.2	1630	35.2	3050
	Outlet pressure ($P_{c,o}$), Pa	0	0	0	0
	Temp. rise (ΔT_c), K	22.75	20.98	21.15	23.61
	Pressure drop (ΔP_c), Pa	21.2	1630	35.2	3050
Overall heat transfer coeff. (U), W/m^2K		348.0	3148.0	379.5	4340.9

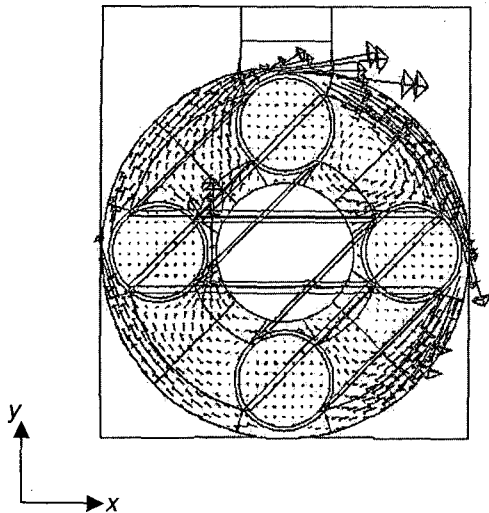


Fig. 7 Velocity vectors on a cross-sectional plane - with spiral baffle ($Z=0.19$)

increases the heat transfer between the tube-side and the shell-side.

Table 4 summarizes results for the shell-and-tube heat exchanger with conventional baffle and spiral baffle. The sizes of tube and shell and the boundary conditions are all the same. The number of baffles is 7 for both cases. The overall heat

transfer coefficient is calculated as follows.

$$U = Q / A \Delta T_{lm} \tag{7}$$

where Q is heat transfer rate, ΔT_{lm} is log mean temperature difference, and A is the surface area of the tubes.

As seen in Table 4, heat transfer is enhanced for the heat exchanger with spiral baffle plates compared with the conventional heat exchanger. This is explained by the elimination of stagnation area in the shell side due to the spiral baffle plates causing rotational flow in the shell side. The 9% higher overall heat transfer coefficient for laminar flow, and 38% for turbulent flow are observed with spiral baffle plates. Tube-side pressure drops are negligibly small for both cases, however, shell-side pressure drop of spiral baffle case is greater than that of conventional baffle case due to the increased shell side fluid velocity. At the present model, heat transfer enhancement for the heat exchanger with spiral baffle plates compared with the conventional heat exchanger is not so large as expected because only one tube and four tube passes system is assumed for the convenience of modeling and computation time. However, it is expected that heat transfer will be enhanced more

considerably when the number of tubes increases.

4. Conclusions

Three-dimensional numerical analyses are performed for the shell-and-tube heat exchangers with spiral baffle plates and conventional vertical baffle plates using the commercial CFD program, CFX4.2. Shell- and tube-side flow fields, pressure drop, and heat transfer performance are analyzed. The results of the shell-and-tube heat exchanger with spiral baffle plates are compared with those of the conventional shell-and-tube heat exchanger. The results show that

(1) The shell-and-tube heat exchanger with spiral baffle plates improves heat exchanger performance because rotational flow in the shell caused by the spiral baffle plates eliminates the stagnation area of the conventional heat exchanger.

(2) Spiral baffle plates introduce vortices in the shell side flow field and enhances heat transfer between shell and tube side fluids, even though it increases pressure drop significantly.

Acknowledgments

The authors wish to thank the support of the BK 21 in Dong-Eui University.

References

- AEA Technology, 1997, *CFX-4.2 Manual*, United Kingdom.
- Gay, B., Mackley, N. V. and Jenkins, J. D., 1976, "Shell-Side Heat Transfer in Baffled Cylindrical Shell-and-Tube Heat Exchangers - An Electrochemical Mass Transfer Modeling Technique," *Int. J. of Heat and Mass Transfer*, Vol. 19, pp. 995~1002.
- Incropera, F. P. and DeWitt, D. P., 1996, *Fundamentals of Heat and Mass Transfer*, 4th ed., John Wiley & Sons Inc., New York.
- Lee, K. S., Chung, J. Y. and Yoo, J. H., 1998, "Thermal and Flow Analysis for the Optimization of a Parallel Flow Heat Exchanger," *Transactions of KSME*, Part B, Vol. 22, No. 2, pp. 229~239.
- Lee, K. S. and Kim, W. S., 1999, "The Effects of Design and Operating Factors on the Frost Growth and Thermal Performance of a Flat Plate Fin-Tube Heat Exchanger Under the Frosting Condition," *KSME International Journal*, Vol. 13, No. 12, pp. 973~981.
- Lee, S. C., Cho, J. W. and Nam, S. C., 1997, "Effect of Baffle Parameters on Heat Transfer in Shell-and-Tube Heat Exchangers," *Transactions of KSME, Part B*, Vol. 21, No. 1, pp. 185~194.
- Lee, S. H., Nam, S. C. and Ban, T. G., 1998, "Performance of Heat Transfer and Pressure Drop in a Spirally Indented Tube," *KSME International Journal*, Vol. 12, No. 5, pp. 917~925.
- Li, H. and Kottke, V., 1998a, "Effect of the Leakage on Pressure Drop and Local Heat Transfer in Shell-and-Tube Heat Exchanger for Staggered Tube Arrangement," *Int. J. of Heat and Mass Transfer*, Vol. 41, No. 2, pp. 425~433.
- Li, H. and Kottke, V., 1998b, "Effect of Baffle Spacing on Pressure Drop and Local Heat Transfer in Shell-and-Tube Heat Exchanger for Staggered Tube Arrangement," *Int. J. of Heat and Mass Transfer*, Vol. 41, No. 10, pp. 1303~1311.
- Patankar, S. V., 1980, *Numerical Heat Transfer and Fluid Flow*, Hemisphere Publishing Co., Washington.
- Prithiviraj, M. and Andrews, M. J., 1998a, "Three Dimensional Numerical Simulation of Shell-and-Tube Heat Exchangers, Part I : Foundation and Fluid Mechanics," *Numerical Heat Transfer, Part A*, Vol. 33, pp. 799~816.
- Prithiviraj, M. and Andrews, M. J., 1998b, "Three Dimensional Numerical Simulation of Shell-and-Tube Heat Exchangers, Part II : Heat Transfer," *Numerical Heat Transfer, Part A*, Vol. 33, pp. 817~828.
- Shah, R. K. and Pignotti, A., 1997, "Influence of a Finite Number of Baffles on Shell-and-Tube Heat Exchanger Performance," *Heat Transfer Engineering*, Vol. 18, No. 1, pp. 82~94.
- Sparrow, E. M. and Reifschneider, L. G., 1986, "Effect of Interbaffle Spacing on Heat Transfer and Pressure Drop in a Shell-and-Tube Heat

Exchanger," *Int. J. of Heat and Mass Transfer*, Vol. 29, No. 11, pp. 1617~1628.

Van Doormaal, J. P. and Raithby, G. D., 1984, "Enhancements of the SIMPLE Method for Predicting Incompressible Fluid Flows," *Numer-*

ical Heat Transfer, Vol. 7, pp. 147~163.

Walker, G., 1990, *Industrial Heat Exchangers - A Basic Guide*, 2nd ed., Hemisphere Publishing Co., New York.